Title
Spatial patterns and source attribution of urban methane in the Los Angeles Basin

Journal
Journal of Geophysical Research: Atmospheres, 121(5)

ISSN
2169-897X

Authors
Hopkins, Francesca M
Kort, Eric A
Bush, Susan E
et al.

Publication Date
2016-03-16

DOI
10.1002/2015jd024429

Peer reviewed

AGU PUBLICATIONS

JGR

Journal of Geophysical Research: Atmospheres

RESEARCH ARTICLE
10.1002/2015JD024429

Key Points:
- Atmospheric methane levels are highly variable across Los Angeles
- The majority of Los Angeles methane emissions are from fossil sources
- Mobile laboratory approach can identify and apportion methane emissions regionally

Supporting Information:
- Supporting Information S1
- Map S1
- Data Set S1

Correspondence to:
F. M. Hopkins,
fhopkins@uci.edu

Citation:
Hopkins, F. M., E. A. Kort, S. E. Bush, J. R. Ehleringer, C.-T. Lai, D. R. Blake, and J. T. Randerson (2016), Spatial patterns and source attribution of urban methane in the Los Angeles Basin, *J. Geophys. Res. Atmos.*, *121*, doi:10.1002/2015JD024429.

Received 3 NOV 2015
Accepted 17 FEB 2016
Accepted article online 20 FEB 2016

Spatial patterns and source attribution of urban methane in the Los Angeles Basin

Francesca M. Hopkins[1,2], Eric A. Kort[3], Susan E. Bush[4], James R. Ehleringer[4,5], Chun-Ta Lai[6], Donald R. Blake[7], and James T. Randerson[1]

[1]Department of Earth System Science, University of California, Irvine, California, USA, [2]Now at Jet Propulsion Laboratory, California Institute of Technology, Pasadena, CA, USA, [3]Department of Atmospheric, Ocean, and Space Sciences, University of Michigan, Ann Arbor, Michigan, USA, [4]Department of Biology, University of Utah, Salt Lake City, Utah, USA, [5]Global Change and Sustainability Center, University of Utah, Salt Lake City, Utah, USA, [6]Department of Biology, San Diego State University, San Diego, California, USA, [7]Department of Chemistry, University of California, Irvine, California, USA

Abstract Urban areas are increasingly recognized as a globally important source of methane to the atmosphere; however, the location of methane sources and relative contributions of source sectors are not well known. Recent atmospheric measurements in Los Angeles, California, USA, show that more than a third of the city's methane emissions are unaccounted for in inventories and suggest that fugitive fossil emissions are the unknown source. We made on-road measurements to quantify fine-scale structure of methane and a suite of complementary trace gases across the Los Angeles Basin in June 2013. Enhanced methane levels were observed across the basin but were unevenly distributed in space. We identified 213 methane hot spots from unknown emission sources. We made direct measurements of ethane to methane (C_2H_6/CH_4) ratios of known methane emission sources in the region, including cattle, geologic seeps, landfills, and compressed natural gas fueling stations, and used these ratios to determine the contribution of biogenic and fossil methane sources to unknown hot spots and to local urban background air. We found that 75% of hot spots were of fossil origin, 20% were biogenic, and 5% of indeterminate source. In regionally integrated air, we observed a wider range of C_2H_6/CH_4 values than observed previously. Fossil fuel sources accounted for 58–65% of methane emissions, with the range depending on the assumed C_2H_6/CH_4 ratio of source end-members and model structure. These surveys demonstrated the prevalence of fugitive methane emissions across the Los Angeles urban landscape and suggested that uninventoried methane sources were widely distributed and primarily of fossil origin.

1. Introduction

Methane (CH_4) is an important atmospheric pollutant: the second largest contributor to global warming and a key constituent regulating CO and O_3 [*Cicerone and Oremland*, 1988]. Most sources of CH_4 to the atmosphere have been identified; however, their relative importance to the global budget is uncertain [*Kirschke et al.*, 2013]. CH_4 source budgets are even more uncertain at continental and regional scales [e.g., *Kort et al.*, 2008; *Miller et al.*, 2013]. The majority (50–65%) of CH_4 emissions globally come from anthropogenic sources, with a flux of approximately 330 Tg CH_4 per year [*Kirschke et al.*, 2013]. Reduction of CH_4 emissions has been suggested to be an effective short-term strategy to reduce global warming because of CH_4's high radiative forcing relative to CO_2, around 28 times on a mass basis over a 100 year time horizon [*Shindell et al.*, 2012; *Myhre et al.*, 2013]. However, mitigation of anthropogenic CH_4 emissions requires an accurate CH_4 budget, including knowledge of location and sectoral contributions of different CH_4 emitters, particularly at scales where mitigation policies may be enacted [*Hsu et al.*, 2010; *Jeong et al.*, 2013].

Observations of elevated CH_4 levels in cities demonstrate that significant emissions of anthropogenic CH_4 are derived from urban areas [*Blake et al.*, 1984; *Wunch et al.*, 2009]. According to inventory estimates, 35% of the anthropogenic CH_4 in North America is emitted from urban regions [*Marcotullio et al.*, 2013]. However, recent atmospheric studies at the state and city levels in California suggest a 30–80% underestimation of CH_4 emissions in the state greenhouse gas inventory, using stationary and airborne trace gas measurements [*Wunch et al.*, 2009; *Hsu et al.*, 2010; *Wennberg et al.*, 2012; *Jeong et al.*, 2013; *Peischl et al.*, 2013; *Wong et al.*, 2015]. Uncounted fugitive emissions, such as leaks from natural gas pipelines, are hypothesized to account for this mismatch between bottom-up inventories and top-down measurements [*Brandt et al.*, 2014]. On-road surveys in major cities such as Boston and Washington, DC have revealed large fugitive leaks from natural gas distribution

pipelines [*Phillips et al*., 2013; *Jackson et al*., 2014]. In addition to extensive natural gas pipeline networks, cities have a variety of other CH_4 sources, including landfills, water treatment plants, natural gas vehicles, and infrastructure, and in the case of Los Angeles, fossil fuel extraction and refining and dairy agriculture. Fugitive emissions may also originate from these sectors. The heterogeneous mixture of source sectors in the urban environment complicates stationary and aircraft measurements of trace gases that cannot resolve fine-scale structure at the source level. Extensive road networks in cities enable vehicle coverage over large areas, providing a method for measuring the spatial distribution of CH_4 emissions. On-road sampling of surface trace gas enhancement can locate CH_4 emission hot spots and attribute CH_4 enhancements to source sectors and aid in interpretation of stationary or remotely sensed measurements [e.g., *Petron et al*., 2012; *Leifer et al*., 2013].

In the U.S., the two largest sources of urban CH_4 emissions are waste disposal and natural gas systems [*U.S. Environmental Protection Agency* (*US EPA*), 2014]. These two sources represent the two primary pathways by which CH_4 is produced—biogenic and thermogenic. Waste disposal, in landfills and wastewater treatment plants, produces biogenic CH_4 as a result of microbial decomposition of organic matter under anaerobic conditions. Biogenic CH_4 is also produced in the gut of livestock and from manure. In contrast, thermogenic CH_4 originates from the geologic processes that create all fossil fuels and is present in fossil fuel deposits including coal beds, oil fields, and geologic seeps [*Etiope and Ciccioli*, 2009]. Thermogenic CH_4 is also emitted through intentional venting and fugitive leaks in the extraction, storage, refining, transport, and use of natural gas. Incomplete combustion of fuels represents a third pathway for CH_4 production; pyrogenic sources are also a minor component ($<$2%) of CH_4 emissions [*US EPA*, 2014]. Both thermogenic and pyrogenic sources of CH_4 also emit more complex hydrocarbons, including ethane (C_2H_6), whereas biogenic sources do not [*Rudolph*, 1995; *Kirchstetter et al*., 1996; *Etiope and Ciccioli*, 2009]. Hence, elevated CH_4 accompanied by elevated C_2H_6 values can be used as a tracer of fossil fuel sources of CH_4 [e.g., *Aydin et al*., 2011].

In the Los Angeles Basin, evidence from stable isotopes of CH_4 and measurements of higher hydrocarbons (e.g., C_2H_6, propane, and butane) suggest that fossil emissions are the predominant source of CH_4 [*Townsend-Small et al*., 2012; *Wennberg et al*., 2012; *Peischl et al*., 2013]. Specifically, leakage from natural gas infrastructure [*Wennberg et al*., 2012] and from local fossil CH_4 sources [*Peischl et al*., 2013] are thought to be the most important contributors. However, the complex geologic setting and intense human impact within the basin complicate CH_4 source attribution in the Los Angeles area. The Los Angeles region is known for naturally occurring geologic seeps, such as the La Brea Tar Pits, as well as extensive oil drilling taking place during the last century and continuing to the present day [*Bilodeau et al*., 2007]. In addition, Los Angeles is a major industrial and shipping center, with more than 10 oil refineries and storage facilities. The number of producing wells in the basin has decreased since the 1960s; however, the number has increased anew over the past decade with application of enhanced oil recovery techniques such as hydraulic fracturing [*Cardno ENTRIX*, 2012; *Gautier et al*., 2012; *Tennyson*, 2005]. Industrial centers, such as the Port of Los Angeles, the Harbor area, the surroundings of Los Angeles International Airport, and downtown, were constructed near or over major oil fields (Figure 1a) meaning that many anthropogenic sources of CH_4 are colocated with each other and with potential geologic CH_4 sources.

Missing from stationary or airborne measurements is detailed spatial information about the distribution of CH_4 sources that is needed for developing monitoring and mitigation strategies for urban CH_4 emissions. Here we present data from an extensive on-road survey of CH_4 levels in the Los Angeles Basin during June 2013. Our goals were twofold: to describe the spatial patterns of CH_4 and other trace gases with urban sources in the Los Angeles Basin and to use local measurements of the C_2H_6 to CH_4 ratio to attribute sources of fugitive CH_4 emissions, measured as hot spots and in local background air. We demonstrate the utility of mobile surveys to locate and attribute urban CH_4 hot spots, and of complementary measurements of C_2H_6, to perform a regional source apportionment.

2. Methods

2.1. Instrumentation

We used a mobile observatory system to continuously survey trace gas mole fractions on-road while also recording global position and winds. The platform was a 2011 Ford Transit Connect van with a modified

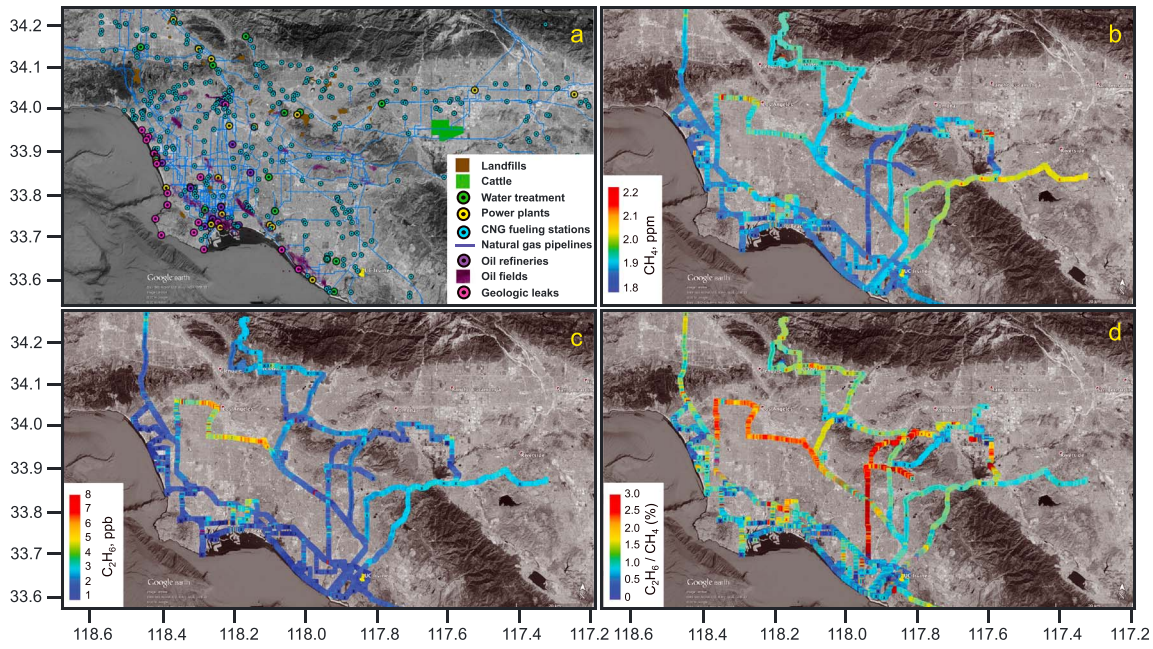

Figure 1. Map of Los Angeles Basin methane sources and sampling area for June 2013 campaign. Map depicts 33.6° to 34.3°N and 117.3° to 118.7°W. (a) Location of major CH_4 sources in the basin. Individual sources include the following: oil refineries (purple markers), oil wells (small magenta circles), geologic seeps (magenta markers), active and former landfills (brown shaded areas), wastewater treatment (green markers), cattle (green shaded area), power plants (yellow markers), natural gas pipelines (blue lines) and natural gas fueling stations (cyan markers). (b) Daytime measurements of CH_4 mole fraction, in parts per million. (c) Daytime measurements of C_2H_6 mole fraction, in parts per billion. (d) Daytime measurements of the ratio of C_2H_6 to CH_4 expressed as mole ratio percent.

electrical system and sampling mast that extended to 3.5 m above the road surface located just behind the driver's seat of the vehicle [*Bush et al.*, 2015].

The observatory was equipped with two cavity ring-down spectrometers (Picarro Inc., Sunnyvale, California), one measuring CH_4, CO_2, and H_2O (G1301) and the other measuring CO, CO_2, and H_2O (G1302). The instruments were plumbed in serial, sampling air from a common inlet located at the top of the sampling mast. Outside air was pumped continuously through the line at a rate of 4.2 L/min. The G1301 reported measurements every 2–3 s and the G1302 every 3–4 s. The time delay for measurement of outside air ranged from 0.7 to 3 s, depending on the variable instrument sampling rate. During this campaign, the laboratory also had an Aerodyne Ethane Mini Monitor quantum cascade laser spectrometer on board to measure C_2H_6 and CH_4 [*Yacovitch et al.*, 2014]. The Ethane Mini Monitor sampled from a separate inlet line to enable instrument background scans by purging with N_2 for 30 s every 15 min. In addition, the instrument measured a reference C_2H_6 cell for 3 s every 2 min to maintain a line lock on the C_2H_6 spectral feature. Apart from reference and background scan times, data were collected once a second, with a 1 s response time.

Position data were collected every 5 s by a GPS16X-HVS receiver (Garmin International, Inc., Olathe, Kansas) mounted on the vehicle's roof, and wind direction and speed were measured with a Weather Station WS-200WM (Airmar Technology Corp., Milford, New Hampshire) mounted to the top of the sampling mast.

2.2. Calibration

We calibrated measurements made by cavity ring-down trace gas spectrometer using two NOAA-certified air standards that contained known amounts of CO_2, CO, and CH_4. Standards were measured for several minutes before and after each transect, with each transect defined as a set of on-road measurements made over the course of several hours. The relationship between known and measured standard values was applied as a linear correction to the data collected during that transect. Measurement precision was 1.7 ppm for CO_2, 2.1 ppb for CH_4, and 8 ppb for CO based on the standard deviation of all measured standards for the campaign. For CH_4, G1301 performance was found to be linear over a range of standard values from 1.7 to 10 ppm. Reported CH_4 values greater than 10 ppm hence represent an approximation ($<$0.01% of data reported here).

We report C_2H_6 data as spectroscopic mole fraction, which has an expected 1 s precision of 0.1 ppb on a moving mobile laboratory platform [*Yacovitch et al*., 2014]. We checked the accuracy of spectroscopic C_2H_6 by comparing it to C_2H_6 measured in the laboratory on five simultaneous whole air samples that were taken during periods when atmospheric C_2H_6 was relatively constant. The average of spectroscopic C_2H_6 from the whole air sampling period was within 10% of reported C_2H_6 values by gas chromatography-flame ionization detector [*Colman et al*., 2001].

2.3. Data Processing

Original data were collected at varying frequencies for each instrument ranging from once every second (Aerodyne Mini Monitor) to once every 3–4 s (Picarro G1302). We used correlation analysis of the two CO_2 data streams to adjust for time delays between the two Picarro instruments and CH_4 correlations to adjust for time delays between the Aerodyne Mini Monitor and Picarro G1301. All data were subsequently averaged to 5 s intervals.

For spatial analyses, 5 s averaged data were spatially gridded along 150 m road intervals by averaging observations taken within this increment. The 150 m segments were chosen to maximize the information content of gridded data; less than 3% of the 150 m segments required linear interpolation of the nearest neighbors to fill in gaps in data.

2.4. Background Trace Gas Mole Fractions

We determined urban excess values for each trace gas species by subtracting an estimated clean air background mole fraction from trace gas-enhanced measurements made in polluted urban air, following *Blake et al*. [1984]. We estimated the clean air background value for each trace gas by selecting the minimum observation for each transect in the study period and then averaging the lowest 20% of these transect minimums (i.e., the lowest four out of 21 transects). We estimated the uncertainty in background values as the standard deviation of the minimum trace gas measurement from all transects within the basin ($n = 21$). The background value for CH_4 was 1821 ± 24 ppb, CO was 80 ± 24 ppb, CO_2 was 396.3 ± 3.2 ppm, and C_2H_6 was 0.6 ± 0.2 ppb. Background values measured in the basin were all within 1 standard deviation of values reported at Kumukahi, Hawaii in June 2013 (June 2009 for C_2H_6) by NOAA's Global Greenhouse Reference Network [*Helmig et al*., 2011; *Dlugokencky et al*., 2013a, 2013b; *Novelli and Masarie*, 2013]. At Kumukahi, CH_4 was 1836 ± 7 ppb, CO was 85 ± 5 ppb, and CO_2 was 399.8 ± 0.7 ppm from the average of flask samples on eight measurement days in June 2013, and C_2H_6 was 0.6 ± 0.1 ppb from the average of flask samples from five measurement days in June 2009. The background value for C_2H_6 was similar to observations made from aircraft above the Los Angeles Basin, 0.6 ± 0.3 ppb for the lowest values on three measurement days that coincided with on-road sampling.

2.5. Observations

We sampled approximately 1900 km of road in the Los Angeles Basin, in June and early July of 2013 (Figure 1). We conducted 21 transects, with each transect defined as a set of on-road measurements made within a specific time period (e.g., midday on 15 June). Most routes were repeated a minimum of two times, at midday (10 A.M. to 4 P.M.) and after nightfall (9 P.M. to 1 A.M.).

Transect routes were designed to characterize the C_2H_6/CH_4 ratios of known biogenic and fossil CH_4 sources, including landfills, wastewater treatment facilities, livestock, oil fields, refineries, natural gas storage, distribution infrastructure, and geologic sources (Figure 1a: map image of known CH_4 emitters in Los Angeles Basin). We also designed transect routes to cover common land use types within the Los Angeles Basin, with varying degrees of human influence (urbanization).

On 17–19 June, we coordinated on-road sampling to cover the same locations at approximately the same time as a concurrent aircraft campaign. The aircraft was a DC-8 flown out of NASA's Dryden Flight Research Center over the Los Angeles Basin as part of the NASA Student Airborne Research Program (www.nserc.und.edu/sarp/sarp-2009-2013/2013). During flight, whole air samples were taken in evacuated 2 L stainless steel canisters. Canister samples were analyzed in the laboratory for CH_4, C_2H_6, CO, and CO_2 mole fractions and along with other constituents by gas chromatography-flame ionization detector [*Colman et al*., 2001]. We included only samples taken over land in the Los Angeles Basin at less than 3000 ft (914 m) above ground level in this analysis.

Table 1. Summary of Biogenic CH_4 Hot Spots Associated With Individual Facilities or Sites

Source Type	Facility/Site	Date(s)	Time of Day	Latitude	Longitude	Hot Spot Extent (km)	Average Excess CH_4 (ppm)[a]	Maximum Excess CH_4 (ppb)	Maximum Excess C_2H_6 (ppb)	C_2H_6/CH_4 Slope (%)[b]	Sample Size (n)	R^2 value	p value
Active landfills	Puente Hills	22 June	A.M. and P.M.	34.02	-118.00	10.14	1.5 ± 2.2	2,725	5.9	0.02 ± 0.01	191	0.04	<0.01
	Scholl Canyon	22 June	A.M.	34.16	-118.19	0.92	0.8 ± 0.4	3,159	2.2	0.00 ± 0.01	46	0.04	0.21
	UCI landfill	24 June	A.M.	33.654	-117.86	0.44	0.12 ± 0.03	2,866	0.5	0.00 ± 0.01	33	0.00	0.76
Former lanfills	Palos Verdes landfill	24 June	A.M.	33.79	-118.35	1.39	0.5 ± 0.5	1,392	1.3	-0.03 ± 0.02	28	0.11	0.09
	Cal Compact landfill	19, 23, and 26 June	A.M. and P.M.	33.84	-118.27	1.93	0.4 ± 0.2	1,811	5.6	-0.13 ± 0.08	48	0.02	0.30
Cattle	Chino	18 and 27 June	A.M. and P.M.	33.99	-117.63	8.86	3.8 ± 9.4	13,246	23.4	0.00 ± 0.00	977	0.00	0.84
Water treatment	Mesa Water District colored water treatment plant	14, 15, 19, 22, 23, 24, 26, and 27 June and 5 July	A.M. and P.M.	33.687	-117.914	5.3	0.7 ± 0.5	7,768	4.3	0.02 ± 0.01	137	0.09	<0.01
	Orange County Sanitation District reclamation plant 1	14, 19, 23, 24, 26, and 27 June and 5 July	A.M. and P.M.	33.69	-117.94	2.0	0.3 ± 0.1	1,433	9.9	0.50 ± 0.05	77	0.40	<0.01

[a]Reported error is one standard deviation of the mean.
[b]Slope is calculated by orthogonal distance regression; reported error is the largest of error estimates for slope from orthogonal distance regression and ordinary linear regression.

2.6. Hot Spot Identification

Plumes of air containing CH_4 values that exceeded the 95th percentile of CH_4 observations for that transect were considered indicators of a CH_4 hot spot. Some hot spots coincided with known emission sources (shown in Figure 1a), while others were of an unknown origin. We defined hot spots as road segments where at least one 150 m segment had a CH_4 value that exceeded the 95th percentile threshold (132 to 360 ppb above the local background level). The spatial extent of each hot spot was defined by the number of adjacent 150 m road segments that had CH_4 values above the local background level. Local background CH_4 levels varied over the course of each transect due to spatial variability and diurnal changes in boundary layer height and were thus determined by visual inspection of each transect. We approximated the amount of local CH_4 enhancement by summing excess CH_4 above the local background level (i.e., area under the curve) for each hot spot.

2.7. Source Apportionment

We used the range of mole fraction ratios of excess C_2H_6 to excess CH_4 from known CH_4 emission sources to apportion CH_4 in hot spots of unknown origin, and for local background air measured away from CH_4 hot spots, representing a regional mix of CH_4 source sectors. We used linear regression on excess C_2H_6 and excess CH_4 observations from CH_4 hot spots of known emitters to determine the range of C_2H_6/CH_4 ratios that characterized biogenic and fossil sources. Regression slope estimates included uncertainty in background mole fractions, estimated as 1 standard deviation of background levels [*York et al.*, 2004]. In theory, biogenic sources

Journal of Geophysical Research: Atmospheres

10.1002/2015JD024429

Table 2. Summary of Natural Gas CH_4 Hot Spots Associated With Individual Facilities or Sites

Source Type	Facility/Site	Date(s)	Time of Day	Latitude	Longitude	Hot Spot Extent (km)	Average Excess CH_4 (ppm)[a]	Maximum Excess CH_4 (ppb)	Maximum Excess C_2H_6 (ppb)	C_2H_6/CH_4 Slope (%)[b]	Sample Size (n)	R^2 value	p value
Power plants	Haynes steam plant	14 and 27 June	A.M. and P.M.	33.76	-118.096	15.0	0.07 ± 0.02	312	4.5	3.1 ± 0.5	19	0.24	0.03
	AES Alamitos	22 June	P.M.	33.77	-118.10	0.8	0.27	482	9.7	3.8 ± 0.3	50	0.36	<0.01
	NRG	23 June	A.M.	33.91	-118.425	0.4	0.29	1,256	29.2	2.5 ± 0.7	5	0.61	0.12
CNG fueling stations	Clean Energy headquarters	17, 23, 24, and 26 June	A.M. and P.M.	33.774	-118.077	1.9	0.3 ± 0.4	1,110	30.5	3.1 ± 0.1	38	0.94	<0.01
	Clean Trucks, Port of Long Beach	24 June	A.M.	33.783	-118.222	0.9	2.1 ± 3.0	58,425	479.7	0.87 ± 0.03	141	0.81	<0.01
	Clean Energy Newport Beach	14 June	A.M.	33.632	-117.927	0.6	0.1	203	1.8	1.2 ± 0.3	12	0.35	0.04
	PH[c] landfill truck gas fueling	22 June	A.M.	34.023	-118.028	0.6	2.2	11,365	117.0	0.9 ± 0.1	32	0.49	<0.01
Natural gas pipelines under roads	Pacific Coast Hwy at Superior, NB[d]	5 July	A.M. and P.M.	33.623	-117.939	1.3	0.05 ± 0.01	315	9.5	2.8 ± 0.5	50	0.25	<0.01
	Santa Ana Ave., Costa Mesa	15 June and 5 July	A.M. and P.M.	33.637	-117.911	3.0	0.06 ± 0.03	490	31.1	1.8 ± 0.1	74	0.27	<0.01
	Goldenwest St., Huntington Beach	15 June	A.M.	33.74	-118.007	0.3	0.29	720	16.9	2.1 ± 0.1	56	0.80	<0.01
	Campus and Carlson, Irvine	16 June	A.M.	33.664	-117.851	0.5	0.18	248	3.0	2.1 ± 0.5	5	0.78	0.04
	91 Fwy at Buchanan, Corona	16 June	A.M.	33.895	-117.50	0.9	0.3	316	4.1	1.9 ± 0.6	8	0.96	<0.01

[a]Reported error is one standard deviation of the mean.
[b]Slope is calculated by orthogonal distance regression; reported error is the largest of error estimates for slope from orthogonal distance regression and ordinary linear regression.
[c]PH: Puente Hills.
[d]NB: Newport Beach.

Table 3. Summary of Geologic CH_4 Hot Spots Associated With Individual Facilities or Sites

Source Type	Facility/Site	Date(s)	Time of Day	Latitude	Longitude	Hot Spot Extent (km)	Average Excess CH_4 (ppm)[a]	Maximum Excess CH_4 (ppb)	Maximum Excess C_2H_6 (ppb)	C_2H_6/CH_4 Slope (%)[b]	Sample Size (n)	R^2 value	p value
Oil refineries	Conoco Phillips	24 June	A.M.	33.778	-118.29	0.3	0.24	1,781	38.9	2.8 ± 0.5	11	0.54	<0.01
	BP	23 and 26 June	A.M. and P.M.	33.82	-118.24	2.6	0.24 ± 0.01	347	8.8	3.5 ± 0.4	24	0.45	<0.01
	Exxon	17 June	A.M.	33.85	-118.32	2.4	0.13	559	17.3	4.0 ± 0.2	116	0.64	<0.01
	Chevron	19 and 23 June	A.M.	33.91	-118.40	3.1	0.2 ± 0.2	1,101	9.6	1.1 ± 0.1	69	0.35	<0.01
Oil fields	Newport Beach	14, 15, and 17 June and 5 July	A.M. and P.M.	33.626	-117.946	0.9	0.09 ± 0.03	223	1.7	-0.1 ± 0.1	35	0.00	0.79
	Huntington Beach	15 June	A.M.	33.687	-118.005	2.8	0.09 ± 0.03	352	3.2	1.1 ± 0.2	20	0.47	<0.01
	Seal Beach	14, 17, and 24 June	A.M. and P.M.	33.76	-118.11	1.4	0.2 ± 0.2	623	39.0	7.2 ± 0.6	38	0.48	<0.01
	Long Beach	17, 24, and 26 June	A.M. and P.M.	33.81	-118.17	34	0.3 ± 0.1	855	19.4	2.7 ± 0.1	79	0.75	<0.01
	Santa Fe Springs	22 June	A.M.	33.943	-118.065	1.5	0.08 ± 0.02	1,111	9.9	0.67 ± 0.05	118	0.48	<0.01
	Inglewood	26 June	P.M.	34.00	-118.37	0.2	0.16	653	39.2	9 ± 5	3	0.58	0.45
Geologic seeps	Holmwood and Broad, NB[c]	5 July	A.M. and P.M.	33.626	-117.924	0.4	0.14 ± 0.03	1,352	2.3	0.01 ± 0.02	68	0.01	0.45
	Playa Vista	19 and 23 June	A.M. and P.M.	33.973	-118.421	5.3	5 ± 9	27,201	65.6	0.14 ± 0.01	405	0.70	<0.01
	La Brea tarpits	19 and 26 June	A.M. and P.M.	34.063	-118.355	1.8	1 ± 1	5,021	23,757	4.04 ± 0.08	615	0.58	<0.01

[a] Reported error is one standard deviation of the mean.
[b] Slope is calculated by orthogonal distance regression; reported error is the largest of error estimates for slope from orthogonal distance regression and ordinary linear regression.
[c] NB: Newport Beach.

should have a ratio of 0 (i.e., no concurrent C_2H_6 production). In practice, many primarily biogenic sources had small but significant positive ratios because of measurement uncertainties and a small amount of contribution from nearby or colocated fossil sources. We used the observed range of excess C_2H_6 to excess CH_4, hereafter denoted C_2H_6/CH_4, from known sources to determine the likely origins of unknown hot spots based on their C_2H_6/CH_4 slopes. For regional source apportionment, we included only observations of local background air measured away from CH_4 hot spots, where we assume that the air is well mixed with respect to CH_4 and hence representative of a mixture of urban CH_4 sources across the Los Angeles Basin.

3. Results

3.1. Spatial Distribution of CH_4 and C_2H_6 Across the Los Angeles Basin

CH_4 mole fractions were highly variable across the Los Angeles Basin, ranging from near background levels to 58 ppm measured at the Clean Trucks compressed natural gas (CNG) fueling station in the Port of Long Beach (Figure 1b and Map S1 in the supporting information). We observed local CH_4 enhancement (hot spots) in the vicinity of many known CH_4 emission sources, including active and closed landfills, cattle operations, water treatment facilities, geologic seeps, oil extraction and refining facilities, natural gas infrastructure, and gas-fired power plants (Tables 1–3). We also observed many CH_4 hot spots of an unknown origin, including local enrichment of about five times background levels in a discrete, high CH_4 event. Elevated levels

Table 4. Sectoral CH_4 Hot Spot Characteristics[a]

Source Category	Emitters Sampled	C_2H_6/CH_4 Slope (%)[b]	Percent of the Total Campaign Distance Driven
		Biogenic Sources	
Active landfills	2	0.01 (0.01)	0.4
Former landfills	3	-0.05 (0.08)	0.5
Cattle	1[c]	0.00 (0.00)	1.5
Water treatment	1[d]	0.02 (0.01)	1.1
Biogenic average	**7**[d]	**0.05 (0.03)**	**3.5**
		Fossil Sources: Fugitive Natural Gas Leaks	
Power plants	3	3.1 (0.9)	0.1
CNG fueling stations	4	1.5 (0.3)	0.4
NG pipeline leaks	5	2.1 (0.9)	0.3
Natural gas average	*12*	*2.2 (0.4)*	*0.8*
		Fossil Sources: Geologic Sources and Fossil Fuel Production	
Oil refineries	4	2.9 (0.7)	0.4
Oil drilling	6	3.4 (5.0)	0.6
Geologic leaks	3	1.4 (0.1)	0.7
Geologic source average	*13*	*2.8 (1.4)*	*1.7*
Fossil average	**25**	**2.5 (1.1)**	**2.5**

[a]Sectoral averaged (e.g., biogenic, fossil) shown in bold; source category sub-averages (e.g., natural gas, geologic source) shown in italic.
[b]Slope is calculated as the average of C_2H_6/CH_4 for each emitter sampled; error on slope is propagated from error reported in Table 1.
[c]Single region of cattle influence includes multiple individual dairies.
[d]Excludes one water treatment plant with suspected fossil emissions (Orange County Sanitation District Plant 1).

of atmospheric C_2H_6 were also observed in many, but not all locations where CH_4 enhancements were observed (Figure 1c).

Local CH_4 background levels, excluding known and unknown CH_4 hot spots, varied across the region (Figure 1b). In general, local CH_4 background levels were higher in inland parts of the basin. For example, local background CH_4 levels in Riverside were twice as high as they were in Irvine for the same day, three times as high in Ontario, and four times as high in Pasadena. Inland areas tend to accumulate polluted air generated in the basin due to prevalent onshore winds during spring and summer [e.g., *Vutukuru et al.*, 2006; *Peischl et al.*, 2013]. Local CH_4 levels tended also to be higher in more urbanized areas of the basin, such as near downtown Los Angeles.

C_2H_6 also increased along a coast-to-inland gradient in a manner similar to CH_4, with large areas of enhancement located in downtown Los Angeles, around the Long Beach oil field, and in the city of Ontario (Figure 1c). C_2H_6 mole fractions ranged from background levels similar to those observed in remote ocean regions to 2370 ppb measured at the La Brea Tar Pits. Local background levels of C_2H_6 varied even more than for CH_4, with levels fourfold higher in Riverside and sixfold higher in Pasadena than in Irvine and up to 20 times higher in Ontario. The greater urban enhancements of C_2H_6 compared to CH_4 were likely driven by significant urban C_2H_6 emissions and lower remote background mole fractions as a consequence of a shorter lifetime (approximately 2 months for C_2H_6 versus >10 years for CH_4) and little C_2H_6 production in remote ocean regions [*Xiao et al.*, 2008]. The ratio of C_2H_6 to CH_4 was also highly variable across the region. In particular, C_2H_6/CH_4 was markedly higher along surface streets in dense, highly urbanized areas near downtown Los Angeles and central Orange County (Figure 1d and Map S1).

3.2. C_2H_6/CH_4 Ratio of Known Emitters

We made measurements of CH_4 and C_2H_6 at known CH_4 emission sources to characterize the C_2H_6/CH_4 ratios of biogenic and fossil end-members and to enable subsequent use of this information to apportion CH_4 emission sources in the Los Angeles Basin. We calculated C_2H_6/CH_4 ratios for each known CH_4 emitter and subsequently for each source sector as the slope of a line fit through a plot of excess C_2H_6 versus excess CH_4 using a minimization of orthogonal distance and including measurement error in both variables (Tables 1–3). The C_2H_6/CH_4 ratio for biogenic sources ranged from $-0.05 \pm 0.08\%$ for former landfills to $0.02 \pm 0.01\%$ for water treatment facilities (Table 4). Most biogenic CH_4 emitters did not have statistically significant C_2H_6/CH_4 slopes (i.e., slopes were not statistically different from 0), except for the Puente Hills

landfill and several water treatment facilities (Table 1). Significant C_2H_6/CH_4 slope values were likely caused by collocated fossil emissions. For example, fossil-derived natural gas and biogenic CH_4 may be combined to fuel natural gas vehicles. Both the Puente Hills landfill and the Orange County Sanitation District water treatment plant had CNG fueling stations on site.

Known fossil sources of CH_4 were grouped into two categories based on their expected C_2H_6/CH_4 ratios: (1) fugitive leaks of pipeline-quality natural gas, which include emissions from gas-fired power plants, CNG fueling stations, and natural gas pipelines (Table 2), and (2) unprocessed geologic CH_4 sources, including oil fields, oil refineries, and geologic seeps (Table 3). Previous studies have shown a relatively narrow range of C_2H_6/CH_4 ratios for pipeline natural gas compared to geologic CH_4 sources [*Jeffrey et al*., 1991; *Wennberg et al*., 2012]. Fugitive natural gas leaks for sources sampled in this campaign had C_2H_6/CH_4 ratios ranging from $1.5 \pm 0.3\%$ for CNG fueling stations to $3.1 \pm 0.9\%$ for natural gas-fired power plants (Table 4). Among pipeline gas sources, all C_2H_6/CH_4 slopes were statistically significant at the $p < 0.05$ level except for one power plant sample with few ($n = 5$) measurements (Table 2). This range is consistent with direct measurements of C_2H_6/CH_4 in pipeline gas in Southern California, 1.33–2.59%, reported by *Wennberg et al*. [2012]. C_2H_6/CH_4 ratios for geologic CH_4 sources tended to be higher than those for pipeline gas, ranging from $1.4 \pm 0.1\%$ for geologic seeps to $3.4 \pm 5.0\%$ for oil fields (Table 4). However, the range of C_2H_6/CH_4 ratios for individual geologic sources was very broad, spanning $-0.1 \pm 0.1\%$ to $9 \pm 5\%$ for oil fields and $0.01 \pm 0.02\%$ to $4.0 \pm 0.1\%$ for geologic seeps (Table 3). These C_2H_6/CH_4 values were consistent with previous observations in oil fields, 0.7–12.0%, and geologic seeps, 0.8–7.5%, in the Los Angeles Basin [*Jeffrey et al*., 1991]. Several geologic sources had C_2H_6/CH_4 ratios similar to biogenic sources (e.g., Newport Beach oil field, geologic seeps in Newport Beach, and Playa Vista) and may be due to biodegradation of higher hydrocarbons or mixing of thermogenic and biogenic natural gases, both of which have been observed in the Los Angeles Basin [*Jeffrey et al*., 1991].

3.3. Distribution of CH_4 and Other Trace Gases

Atmospheric levels of trace gases were distributed unevenly across the basin, with high CH_4 (and C_2H_6) values concentrated in CH_4 hot spots (Figure 1). We compared the spatial distributions of the four measured gases with urban sources by their Gini coefficients, where 0 represents a perfectly equal distribution and 1 represents a perfectly unequal distribution [*Gini*, 1912]. CH_4 was the most unevenly distributed trace gas over the basin, with a Gini coefficient of 0.55, followed by C_2H_6, 0.47; CO, 0.42; and CO_2, 0.39.

To better understand patterns of emission variability, particularly for CH_4 hot spots of unknown origin, we removed data collected in CH_4 hot spots associated with known emission sources from further analysis. This subset of data comprised about 5.9% of the total distance covered in the campaign. We then sorted and ranked the remaining 94.1% of the observations according to their contribution to the total excess measured during the campaign (Figure 2). A considerable amount of excess CH_4 measured in the Los Angeles Basin was associated with CH_4 hot spots from unknown sources. Just 1% of the total distance traveled, excluding CH_4 hot spots of known emission sources, accounted for 8% of excess CH_4 measured across the basin. Similarly, the top 5% of distance traveled by CH_4 mole fraction was responsible for 21% of the total excess CH_4. Hot spots also contributed disproportionately to trace gas excess for C_2H_6 and CO; the top 1% of transect increments accounted for 7% of the total excess C_2H_6, and 8% of the total excess CO. CO_2 was the most evenly distributed trace gas, with the top 1% of transect distance with respect to CO_2 accounting for just 4% of the total excess CO_2.

3.4. Variability in Spatial Patterns Over Time

We used repeated measurements of a section of the Pacific Coast Highway between Newport Beach and Seal Beach to determine how spatial patterns in atmospheric trace gas levels varied with time and under different wind conditions. We observed many CH_4 hot spots in the same location across four different sampling days at four different times of day, despite differences in wind speed and direction (Figure 3).

We calculated the correlation coefficient for trace gas mole fractions between the four complete transects to quantify the repeatability of trace gas observations. CH_4 was highly correlated in space among all four transect runs (correlation p values < 0.004), with an average correlation coefficient of 0.24 and a maximum correlation of 0.51 between the afternoon and night transects. These correlations were highly significant, given the large number of 150 m road segments on each transect ($n = 174$). CO_2 was also well correlated among transects, with an average of 0.21 and a maximum correlation coefficient of 0.47 between the noon and

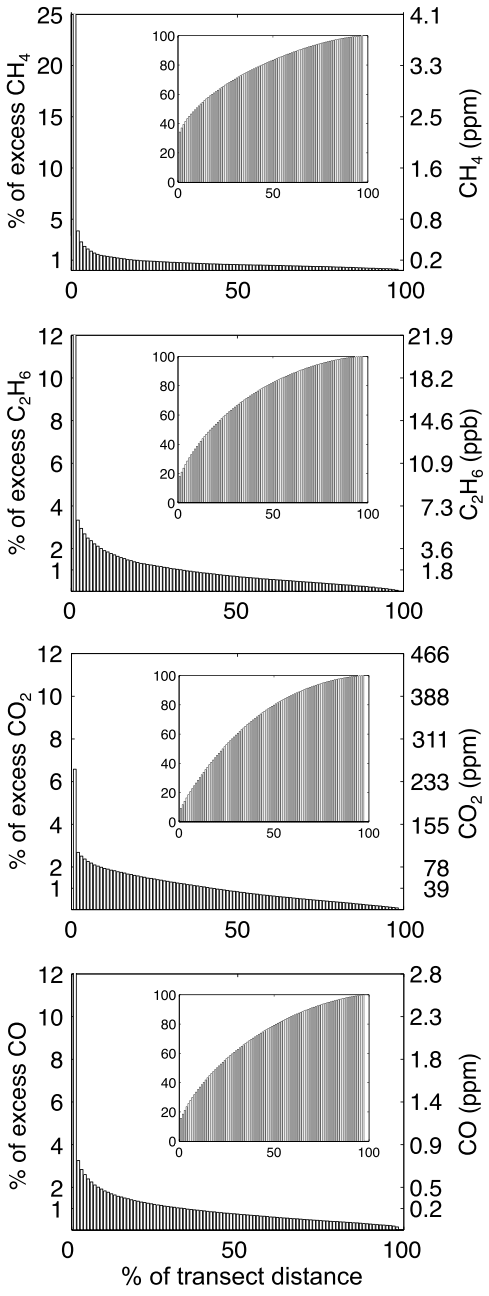

Figure 2. Spatial distribution of urban excess CH_4, C_2H_6, CO_2, and CO by distance. Percent contribution of ordered transect distance to trace gas excess measured over the campaign, excluding data from known CH_4 emission sources. Excess trace gas values for every 150 m road segments were ordered from largest to smallest and binned into increments representing 1% of the total distance driven over the campaign. Bars represent the percent of the total trace gas excess represented by 1% of distance driven (left axis) and corresponding excess value (right axis). Inset plots show cumulative percent of the total excess, starting with the highest 1% of trace gas excess values.

evening transects. CO had the lowest average correlation across transects pairs, with significant correlation observed for only three of six transect combinations ($p < 0.05$). The high spatial correlation of CH_4 values on repeated transects was consistent with emissions from persistent point sources, whereas lower correlations for CO_2 and CO were consistent with more variable traffic emissions.

Trace gas excess mole fractions varied over the course of the day, with a different pattern observed for CH_4 than for CO and CO_2. CH_4 mole fractions were lowest during midday and highest at night. This pattern was consistent with a higher planetary boundary layer and a well-mixed atmosphere in the afternoon that reduced local CH_4 levels and more stable atmospheric conditions at night that trapped CH_4 emissions near the surface. Diurnal patterns of CO and CO_2 were subject to the same boundary layer effect; however, the highest values of CO and CO_2 along this transect were observed in the 5–6 P.M. period, suggesting a time-varying emission source that was consistent with increased vehicle emissions during the evening rush hour.

The lowest trace gas excess values in this section of the Pacific Coast Highway were consistently measured while passing the Bolsa Chica Ecological Reserve, a salt marsh nature preserve (located between km 6 and km 12 of this road section and marked in orange in Figure 3. Reductions in trace gas levels around the marsh were particularly pronounced for CH_4. No CH_4 hot spots were observed in this area, suggesting that CH_4 hot spots originated from built-up urban areas. Despite differences in wind direction and speed among measurement time periods, the consistently low CH_4 mole fractions measured in the vicinity of Bolsa Chica demonstrate the sensitivity of the measurement technique to local emissions and provided qualitative evidence that the measurement footprint of observed hot spots in other parts of the basin was on the order of several kilometers or less.

3.5. Trace Gas Ratios of Unknown Hot Spots and Local Background Air

Both C_2H_6 and CH_4 were unevenly distributed in space; however, some of the locations with the highest CH_4 values were unmatched by C_2H_6 (Figure 4). The top 3% of transect distance with respect to CH_4 values contained 15% of excess CH_4 including unknown hot spots and local background air, but only 10% of excess C_2H_6, suggesting a spatially varying combination of sources across the basin. To visualize this mixture, we calculated the ratio between C_2H_6 and CH_4, and between CO and CO_2 for every 150 m transect segment

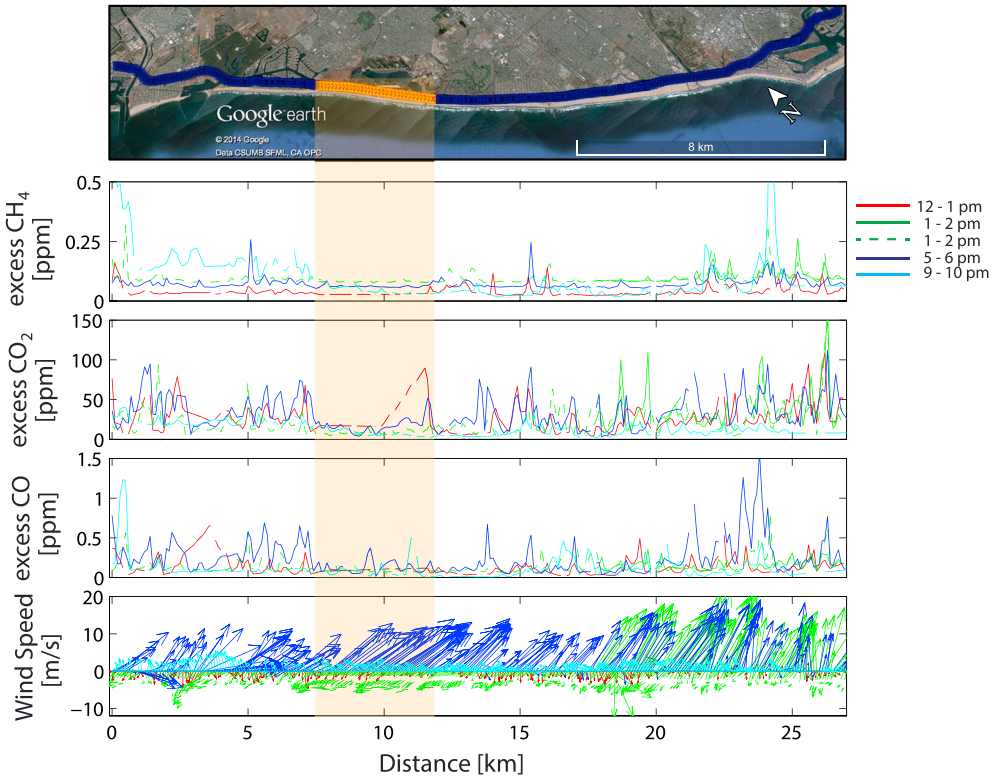

Figure 3. Trace gas excess along a repeated coastal transect. (first panel) Map of route along Pacific Coast Highway beginning at 33.61°N, 117.89°W and ending at 33.76°N, 117.11°W (second panel) Excess CH_4, (third panel) excess CO_2, (fourth panel) excess CO, and (fifth panel) winds, corresponding to the locations shown in the first panel. Trace gas measurements along this transect were made at five different times. Orange highlighted section of map and plots shows section of road passing through a natural reserve (salt marsh), while the remainder of road passed through urbanized land.

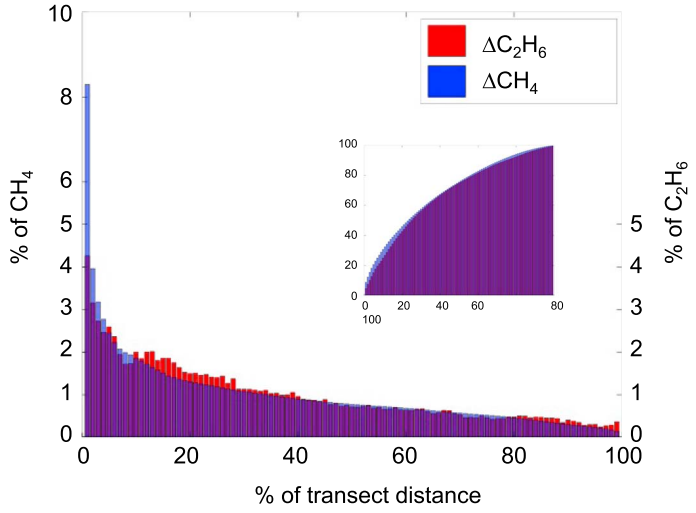

Figure 4. Spatial distribution of CH_4 compared to distribution of C_2H_6 at the same locations. Distribution includes excess CH_4 values in unknown CH_4 hot spots and local background air. Height of bars represents percent of excess CH_4 for each 1% of distance traveled (blue bars) and corresponding percent of excess C_2H_6 for the same locations (red bars).

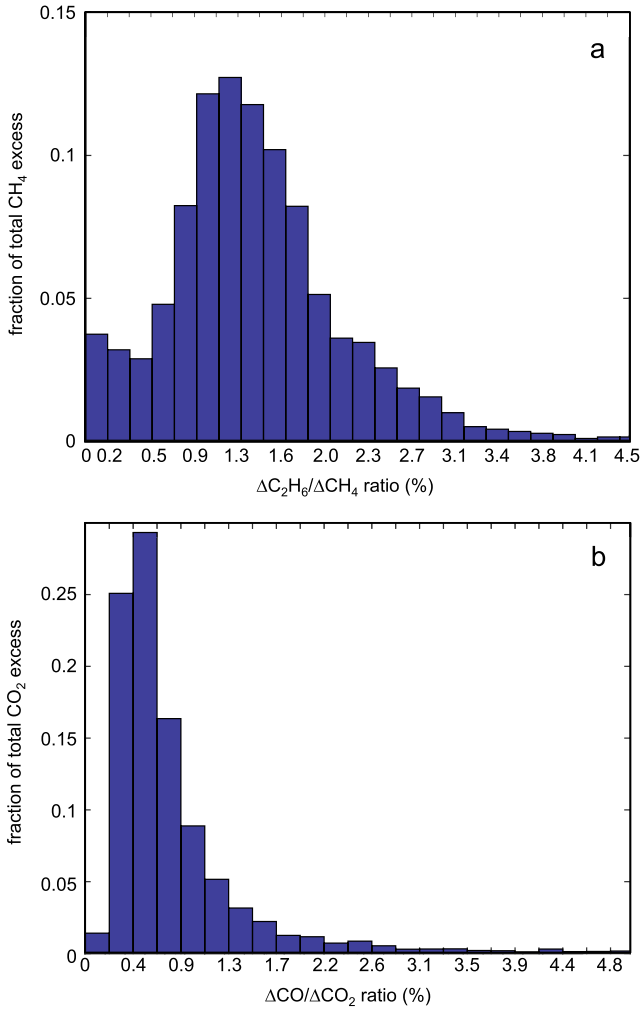

Figure 5. Fossil source tracers for CH_4 and CO_2. (a) Distribution of C_2H_6/CH_4 (mole ratio %) as a fraction of excess CH_4 measured during the June campaign, excluding data from known CH_4 emission sources. (b) Distribution of CO/CO_2 (mole ratio %) as a fraction of the total excess CO_2 measured. The top 5% of CO_2 data with respect to CO/CO_2 values is not shown for scaling reasons.

and plotted the ratios as a fraction of the total CH_4 or CO_2 excess (Figure 5). The bimodal C_2H_6/CH_4 distribution suggests two different source processes contributing to atmospheric CH_4 observations, with a small peak centered on a C_2H_6/CH_4 mole ratio less than 0.5%, reflecting biogenic CH_4 sources, and a second broad peak centered on 1.2%, reflecting fossil CH_4 sources (Figure 5a). Much of the distribution falls along the expected ratio for natural gas in the Los Angeles Basin, 1.33–2.59%, reported by *Wennberg et al.* [2012].

In contrast, a plot of the ratio of CO to CO_2 had only one peak, centered between 0.44% and 0.66% (Figure 5b). This distribution is similar to CO/CO_2 ratios measured in Irvine during the winter of 2007–2008 by *Djuricin et al.* [2010] (0.65–1.0%) and the range observed in Pasadena during summer of 2010 by *Newman et al.* [2013] (0.2–2.0%). Very little excess CO_2 (1%) had a CO/CO_2 ratio less than 0.2%, as would be expected from biogenic CO_2 sources. Hence, the CO/CO_2 ratio suggests that the vast majority of CO_2 measured during the on-road campaign is not representative of terrestrial ecosystem sources, and observed variation was likely driven by combustion sources.

3.6. Source Apportionment of Unknown Hot Spots

We used C_2H_6/CH_4 ratios to apportion excess CH_4 measured at hot spots of unknown origin to biogenic and fossil sources (Figure 6). Unknown CH_4 hot spots, defined as spatially contiguous observations where at least one CH_4 observation exceeded the 95th percentile for that transect with no obvious emission source, comprised 5.8% of the total distance traveled. We used the highest C_2H_6/CH_4 ratio observed for known biogenic sources, 0.50%, as the upper limit for possible C_2H_6/CH_4 ratios from unknown biogenic sources. C_2H_6/CH_4 slopes for CH_4 hot spots falling beneath this value were classified as biogenic. Similarly, we used the lowest C_2H_6/CH_4 excess ratio measured from fugitive natural gas sources, 0.87%, as the lower limit for identifying fossil-derived CH_4 sources. Forty of 213 unknown hot spots were biogenic, 161 were fossil, and 11 had an intermediate slope and hence were considered indistinguishable.

3.7. Source Apportionment of Urban Background Air

The remaining 88.3% of distance traveled, excluding known and unknown CH_4 hot spots, was assumed to represent a more integrated measurement of excess CH_4 sources across the basin. The C_2H_6/CH_4 ratio measured in these samples was similar to that measured by aircraft over the same locations during three days of coincident sampling (Figure 7), $3.1 \pm 0.8\%$ for aircraft versus $3.2 \pm 0.1\%$ for on-road on 17 June, $1.6 \pm 0.3\%$ for aircraft versus $1.4 \pm 0.2\%$ for on-road on 18 June, and $1.7 \pm 1.2\%$ for aircraft versus $2.7 \pm 0.6\%$ for on-road on 19 June. C_2H_6/CH_4

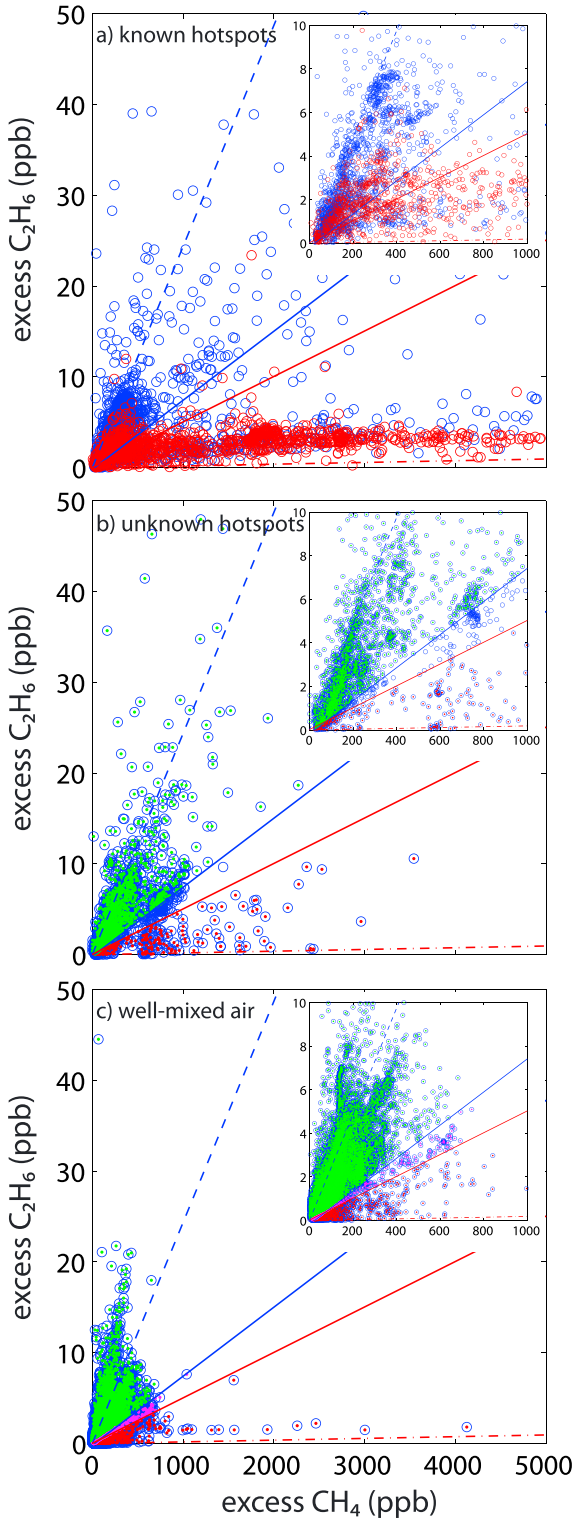

Figure 6. C_2H_6/CH_4 relationship for source apportionment. Excess C_2H_6/CH_4 values for all (a) known hot spots, (b) unknown hot spots, and (c) well-mixed local background air. For known hot spots, data collected at biogenic CH_4 sources are indicated by red dots, and data collected at fossil CH_4 sources are indicated by blue circles. Solid lines show criteria slope values, showing the maximum biogenic slope (red) and minimum fossil slope (blue). Dashed lines are best fit lines for known biogenic (red) and fossil (blue) hot spots. For unknown hot spots and local background air, data are plotted with blue circles. Values attributed to biogenic sources are marked with red dots, and values attributed to fossil sources are marked with green dots. Insets show same data for Figures 6a–6c but at a reduced scale.

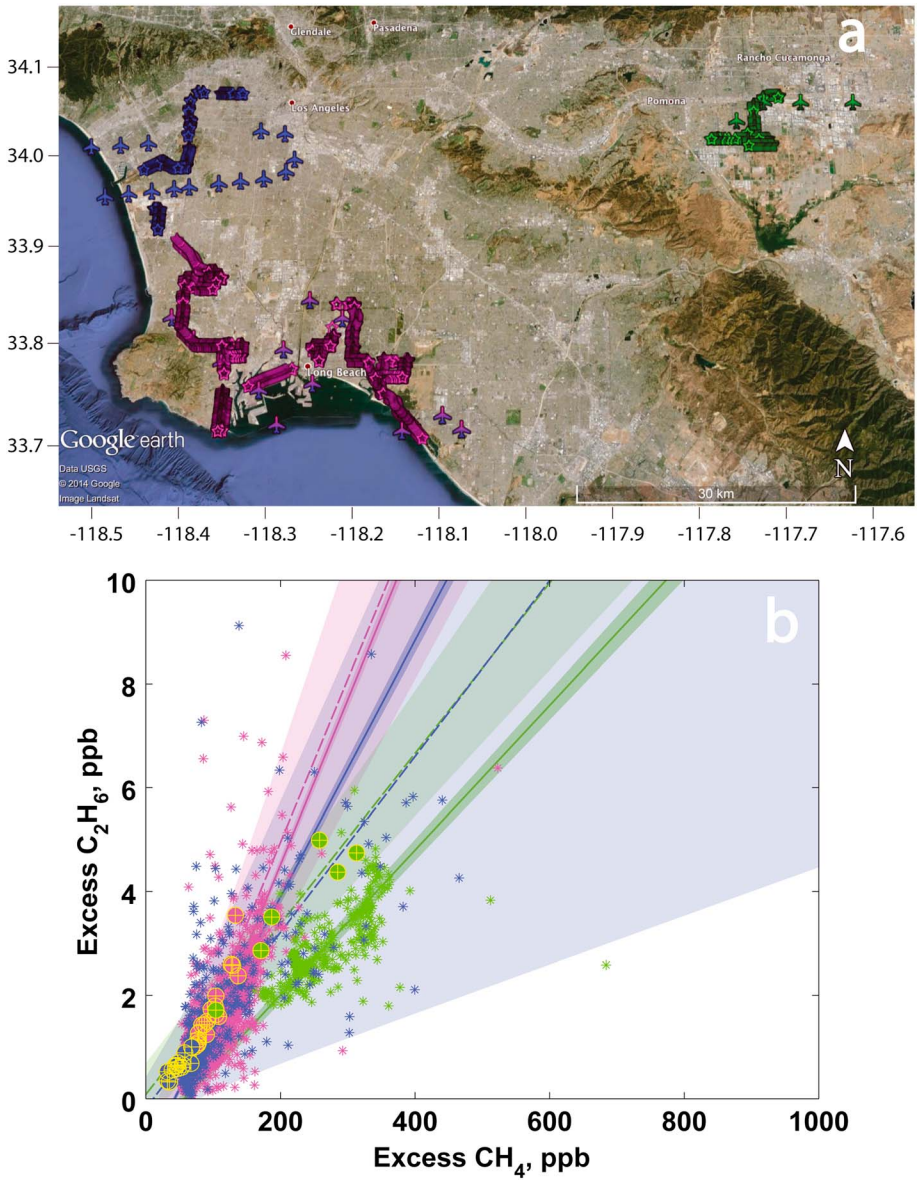

Figure 7. C_2H_6/CH_4 relationship for simultaneous aircraft and on-road sampling. C_2H_6/CH_4 relationship for data collected by aircraft and on-road sampling on 17–19 June 2013, shown in magenta, green, and blue symbols, respectively. (a) A map of on-road sampling (star icons) and aircraft sampling (airplane icons) for each day. (b) The C_2H_6/CH_4 ratios observed on-road (asterisks) and their slope for each sampling day (solid lines), with one standard error of the best fit line shown as the darker shaded area. Aircraft data (colored circles around yellow crosses) and their slopes (dashed line) are also shown with one standard error of the best fit line as lighter shaded area.

values of this well-mixed, local background air were often higher than the minimum C_2H_6/CH_4 ratio observed for natural gas sources, suggesting that most of excess CH_4 present in urban air was fossil derived (Figure 7).

To apportion CH_4 sources in local background air, we compared observed C_2H_6/CH_4 ratios to simulated C_2H_6/CH_4 values for varying proportions of biogenic and fossil CH_4 inputs. We represented C_2H_6/CH_4 values of biogenic sources as a random, normal distribution with a mean of 0% and a standard deviation of 0.03%, based on the average and standard error of C_2H_6/CH_4 values observed at known biogenic hot spots. Similarly, we constructed a normal distribution of C_2H_6/CH_4 values with a mean of 2.5% and standard deviation of 1.1% for fossil sources (Table 4). We determined the fossil fraction that best simulated the observed local background C_2H_6/CH_4 distribution by performing 15,000 mixing trials for each fossil fraction, ranging from 0 to 1, with

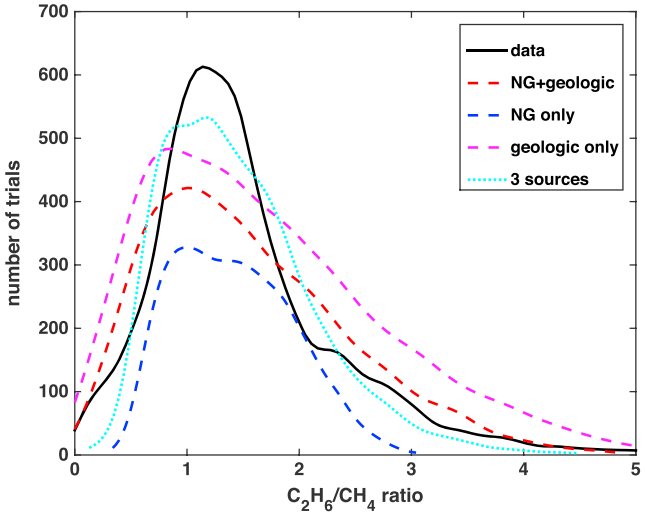

Figure 8. Simulated distributions of C_2H_6/CH_4 ratios for mixing of biogenic and different fossil CH_4 sources. The distribution of the local background air C_2H_6/CH_4 (mole ratio %; after removing known and unknown hot spots) is represented by the black line. The model with two-source mixtures with an average fossil end-member ratio from combined natural gas and geologic sources is shown by a dashed red line, for natural gas sources alone, by a dashed blue line and for geologic sources alone, by a dashed magenta line. A three-source mixture model with separate end-member ratios for biogenic, natural gas, and geologic sources is shown by a dotted cyan line.

end-member ratios randomly selected using the mean and standard deviations of biogenic and fossil emission ration data described above. We found that a mean fossil fraction of 62% (59–64%) best matched C_2H_6/CH_4 values in local background air according to Kolmogorov-Smirnov and Cramer-von Mises test statistics. The range of simulated fossil fraction values includes uncertainty in measured and background CH_4 and C_2H_6 values, by refitting simulations to C_2H_6/CH_4 observations plus or minus propagated error from those sources.

In addition to measurement error, variation in C_2H_6/CH_4 end-member values introduces uncertainty into the inferred fossil fraction. We examined the role of this variation by performing similar simulations to those described above but assuming different fossil end-member C_2H_6/CH_4 values (we do not expect biogenic end-members to differ from 0). Modifying the fossil fraction to reflect only natural gas sources (mean and standard deviation of $2.2 \pm 0.4\%$), the optimal fossil fraction increased to 64%. For the case of only geologic sources (mean and standard deviation of $2.8 \pm 1.4\%$), the inferred fossil fraction decreased to 58%. Nevertheless, neither of these scenarios were able to match the data as well as the fossil end-member that includes both sources (Figure 8). We also separately simulated three hypothesized CH_4 sources: biogenic, natural gas, and geologic, with the same C_2H_6/CH_4 values used in the two-source simulations. The combination of the three sources had a best fit fossil fraction of 65% (Figure 8) and was better able to reproduce the high frequency of C_2H_6/CH_4 values clustered around 1.2%, as well as the large variability in C_2H_6/CH_4 greater than 3%. However, the three-source mixture case is poorly constrained because of the need to fit additional parameters.

4. Discussion

4.1. Methane Source Apportionment in Los Angeles

Mobile laboratory on-road sampling enabled us to make high-frequency, local-scale measurements of multiple trace gases across the Los Angeles Megacity region. We directly measured emission ratios of different sources, at the scale of individual facilities, and simultaneously obtained regionally integrated measurements of multiple trace gases in the urban air mass. Highly spatially resolved CH_4 and C_2H_6 data allowed us to determine the relative contributions of different emission sectors to regional urban CH_4 excess. These data offer further evidence for an under inventoried and dispersed set of fossil CH_4 sources to the Los Angeles atmosphere. We also identified targets for future work and potential mitigation of CH_4 emissions.

We measured CH_4 enrichment at 33 individual point sources to determine the range of C_2H_6/CH_4 ratios for biogenic or fossil sources. As expected, observed C_2H_6/CH_4 of known biogenic sources tended to be very low compared to other observations, despite a few locations with higher than expected C_2H_6 levels (e.g., Orange County Sanitation District Water Reclamation Plant). Known fossil CH_4 emission sources had varied C_2H_6/CH_4 signatures, reflecting the wide range of C_2H_6/CH_4 signatures of geologic sources in the basin. In contrast, local background air had a C_2H_6/CH_4 signature distinct from hot spot biogenic and fossil sources, clearly showing contributions of natural gas and oil sources of CH_4.

Our attribution of 62% of Los Angeles CH_4 to fossil sources, with a possible range of 58–65%, is within the range of other studies using atmospheric C_2H_6/CH_4 measurements in Los Angeles, with estimates of 56% by *Peischl et al*. [2013] and 70% by *Wennberg et al*. [2012]. Our analysis gives insight into why such a large range has been inferred by previous work. First, we found that the inferred contribution of fossil sources depends strongly on the choice of the C_2H_6/CH_4 ratio of the fossil end-member. *Wennberg et al*. [2012] hypothesized that the majority of CH_4 in the Los Angeles Basin originated from leaks of pipeline natural gas and may have overestimated the fossil contribution by assuming that all fossil CH_4 had a C_2H_6/CH_4 ratio representative of natural gas. In contrast to aircraft measurements, our sample of urban air had a much wider range of C_2H_6/CH_4 values that are outside the range of natural gas sources measured here or in previous work in the region [*Wennberg et al*., 2012], demonstrating that fossil CH_4 sources in the Los Angeles Basin must be a mixture of pipeline and unprocessed gas emissions.

Most of the variability in fossil C_2H_6/CH_4 ratios we observed is likely to stem from the large variation in geologic CH_4 sources, which ranged from 0 to 9%. We found that geologic seeps had particularly low C_2H_6/CH_4 values, with two out of three surveyed geologic seeps with C_2H_6/CH_4 values $<0.15\%$. Hence, geologic sources may be confounded for biogenic sources without specific knowledge of the emission source in a particular location. It is possible that the analysis of *Peischl et al*. [2013] underestimated geologic emissions, as some geologic seeps have C_2H_6/CH_4 ratios that are indistinguishable from biogenic sources.

4.2. Strengths and Weaknesses of Mobile Laboratory Technique

Discrepancies between top-down measurements and bottom-up inventories present a major challenge for greenhouse gas mitigation policy and planning, particularly for CH_4. Mobile laboratories are particularly suited for addressing this challenge, having the ability to make complementary regional top-down CH_4 measurements [*Petron et al*., 2012] and facility-level bottom-up measurements [*Jackson et al*., 2014]. In this study, regional C_2H_6/CH_4 apportionment of local background air demonstrated that the predominant source of CH_4 emissions is fossil. We also found that the majority of unknown CH_4 hot spots were of fossil origin, providing further evidence for the importance of dispersed, fugitive fossil CH_4 emissions in the Los Angeles Basin. These CH_4 hot spots of unknown source represent an important target for future research. Repeated measurements of these unknown hot spots are needed to determine whether they persist in time and with tools that can pinpoint the precise locations of CH_4 leaks for source attribution.

Our regional apportionment attributed a large portion of CH_4 in the Los Angeles atmosphere to emissions of pipeline-quality natural gas; however, we observed few discrete leaks from natural gas pipelines. This contrasts with recent observations of frequent pipeline leaks detected by on-road sampling in Boston and Washington, DC [*Phillips et al*., 2013; *Jackson et al*., 2014] and is consistent with recent work showing relatively fewer pipeline gas leaks in the western U.S. [*Lamb et al*., 2015]. Fugitive gas emissions in those cities were found in areas with cast iron gas mains, which are not present in Los Angeles [*Southern California Gas Company*, 2011]. The most significant fugitive emissions of natural gas we observed came from compressed natural gas fueling stations. Fugitive emissions associated with natural gas fueling infrastructure are not currently included in the California Air Resources Board inventory or in prominent life cycle assessment models [*California Air Resources Board*, 2011; A. Burnham, personal communication, 2014]. A better understanding of which components of CNG fueling are leaking is needed for emission quantification and mitigation.

Closed landfill sites also had surprisingly large emissions, with measureable increases in atmospheric CH_4 levels near most sites surveyed (Table 1). Atmospheric CH_4 enhancements were also observed at active and several closed landfill sites that had landfill gas mitigation systems in place, suggesting that the effectiveness of these mitigation activities needs to be verified by atmospheric measurement.

While we were able to make facility-level measurements to identify sources and C_2H_6/CH_4 ratios of urban CH_4 emissions, we acknowledge that a major drawback to on-road sampling is the challenge of making representative measurements. Local atmospheric CH_4 levels strongly depend on proximity to emission source; however, we were not always able to directly access CH_4 emitting facilities, such as inside oil refineries or on landfill surfaces. Here we used measurements away from CH_4 emission sources (local background air) to overcome the limitations of our sampling approach. For this reason, quantitative flux estimates from mobile laboratory sampling in urban areas are extremely challenging. Future studies can reduce this bias by combining multiple techniques along with on-road sampling, including continuous measurement from

tall towers, aircraft, and total column trace gas measurements along with direct flux measurements such as chambers or eddy covariance. Another potential bias in our sample may be due to more extensive coverage in the western portions of the basin, which are densely populated and have the most concentrated oil and gas infrastructure.

Mobile laboratory sampling has significant cost and logistic advantages over aircraft. Unlike aircraft, mobile measurements are also able to target specific CH_4 sources and observe a variety of source mixtures. Nevertheless, proximity to emission sources can also be a disadvantage. Aircraft and remote sensing studies can use the relationship between CH_4 and CO or CO_2 in regionally representative air masses, along with inventories of those gases to estimate CH_4 emissions [e.g., *Wennberg et al*., 2012; *Wong et al*., 2015]. With on-road sampling, however, we found poor relationships between CH_4 and CO, and CH_4 and CO_2, even in well-mixed local background air, likely due to our proximity to on-road sources of CO and CO_2. We found no evidence of vehicle emissions on our CH_4 and C_2H_6 measurements. No CH_4 hot spots coincided with areas of high traffic emissions, including roadway tunnels.

4.3. Urban Pattern of CH_4 (and C_2H_6) Distinct From CO and CO_2

The differing spatial patterns of these four long-lived trace gases demonstrate that different measurements, monitoring, and mitigation approaches are needed for different urban greenhouse gases. Excess CH_4 was relatively concentrated in space compared to CO_2, and large CH_4 enhancement measured in the vicinity of the strongest hot spots suggests that they contribute significantly to basin-wide CH_4 emissions. It may be easier for mitigation efforts to target these point emission sources to achieve equivalent reduction in radiative forcing as reducing more diffuse CO_2 emissions from a whole system. More work is needed to quantify the relative importance of emissions from these CH_4 hot spots.

In addition to monitoring hot spots, the discrepancy between inventory and atmospheric measurement also suggests that wide-ranging measurements must also be made to capture the effects of distributed CH_4 sources. We observed basin-wide enhancement of atmospheric CH_4 levels, a so-called urban dome, but found that the distribution of CH_4 within the city is more strongly controlled by proximity to myriad emission sources. The mobile laboratory approach demonstrated that these points of emission can be linked with individual emitters and attributed to anthropogenic sources. The repeatability of hot spot locations suggests that there are significant, discrete CH_4 emission sources that can be targeted by mitigation efforts. Future work is needed to determine the mechanisms of these leaks (e.g., pipeline seam weld leaks versus fitting leaks), the cost of repair, and an effective strategy for reducing the most critical CH_4 sources. Finally, the fine spatial scales of 10 s to 100 s of meters at which CH_4 hot spots occur suggest that a mobile sampling strategy should be an integral part of a city- or regional-scale greenhouse gas measurement effort.

Acknowledgments
Original geolocated, time-stamped trace gas measurements made by mobile laboratory are provided as Data Set S1. This research is funded by the U.S. Department of Energy's Office of Science (BER) under grant DE-SC0005266. This work was supported in part by the W. M. Keck Institute for Space Studies. We thank Valerie Carranza, Joshua Miu, Mariela Ruacho, Kristal Verhulst, Josette Marrero, and Tianyang Zhu for help with field work and Simone Meinardi for help in the laboratory.

References

Aydin, M., K. R. Verhulst, E. S. Saltzman, M. O. Battle, S. A. Montzka, D. R. Blake, Q. Tang, and M. J. Prather (2011), Recent decreases in fossil-fuel emissions of ethane and methane derived from firn air, *Nature*, *476*, 198–201.

Bilodeau, W. L., S. W. Bilodeau, E. M. Gath, M. Oborne, and R. J. Proctor (2007), Geology of Los Angeles, California, United States of America, *Environ. Eng. Geosci*., *13*(2), 99–160.

Blake, D. R., V. H. Woo, S. C. Tyler, and F. S. Rowland (1984), Methane mole fractions and source strengths in urban locations, *Geophys. Res. Lett.*, *11*, 1211–1214.

Brandt, A. R., et al. (2014), Methane leaks from North American natural gas systems, *Science*, *343*, 733–735.

Bush, S. E., F. M. Hopkins, J. T. Randerson, C. T. Lai, and J. R. Ehleringer (2015), Design and application or a mobile ground-based observatory for continuous measurements of atmospheric trace-gas and criteria pollutant species, *Atmos. Meas. Tech.*, *8*, 3481–3492.

California Air Resources Board (2011), California greenhouse gas emissions inventory, California Air Resources Board Staff Rep. [Available at http://www.arb.ca.gov/cc/inventory/inventory.htm,document:ghg_inventory_by_ipcc_00-09_2011-10-26.xls.]

Cardno ENTRIX (2012), Hydraulic fracturing study, PXP Inglewood oil field report, 206 pp., Plains Exploration & Production Company and Los Angles County, Department of Regional Planning, Los Angeles, Calif.

Cicerone, R. J., and R. S. Oremland (1988), Biogeochemical aspects of atmospheric methane, *Global Biogeochem. Cycles*, *2*, 299–327.

Colman, J. J., A. L. Swanson, S. Meinardi, B. C. Sive, D. R. Blake, and F. S. Rowland (2001), Description of the analysis of a wide range of volatile organic compounds in whole air samples collected during PEM—Tropics A and B, *Anal. Chem*., *73*, 3723–31.

Djuricin, S., D. E. Pataki, and X. Xu (2010), A comparison of tracer methods for quantifying CO2 sources in an urban region, *J. Geophys. Res.*, *115*, D11303, doi:10.1029/2009JD012236.

Dlugokencky, E. J., P. M. Lang, K. A. Masarie, A. M. Crotwell, and M. J. Crotwell (2013a), Atmospheric carbon dioxide dry air mole fractions from the NOAA ESRL carbon cycle cooperative global air sampling network, 1968–2012, Version: 2013-08-2. [Available at ftp://aftp.cmdl.noaa.gov/data/trace_gases/co2/flask/surface/co2_kum_surface-flask_1_ccgg_event.txt.]

Dlugokencky, E. J., P. M. Lang, A. M. Crotwell, K. A. Masarie, and M. J. Crotwell (2013b), Atmospheric methane dry air mole fractions from the NOAA ESRL carbon cycle cooperative global air sampling network, 1983–2012, Version: 2013-08-28. [Available at ftp://aftp.cmdl.noaa.gov/data/trace_gases/ch4/flask/surface/ch4_kum_surface-flask_1_ccgg_event.txt.]

Etiope, G., and P. Ciccioli (2009), Earth's degassing: A missing ethane and propane source, *Science*, *323*, 478.

Gautier, D. L., M. E. Tennyson, R. R. Charpentier, T. A. Cook, and T. R. Klett (2012), Foregone oil in the Los Angles Basin: Assessment of remaining petroleum in giant fields of Southern California Search and Discovery, Article #20164.

Gini, C. (1912), Variabilitá e mutabilitá, in *Memorie di Motodologica Statistica*, edited by E. Pizetti and T. Salvemini, 156 pp., Libreria Eredi Virgilio Veschi, Rome.

Helmig, D., Hueber J., and Tans P. (2011), Non-methane hydrocarbons from the NOAA ESRL surface network, 2004–2011. [Available at ftp://aftp.cmdl.noaa.gov/data/trace_gases/voc/c2h6/flask/event/kum_01D0_event.c2h6.]

Hsu, Y.-K., T. VanCuren, S. Park, C. Jakober, J. Herner, M. FitzGibbon, D. R. Blake, and D. D. Parrish (2010), Methane emissions inventory v-erification in Southern California, *Atmos. Environ.*, *44*, 1–7.

Jackson, R. B., A. Down, N. G. Phillips, R. C. Ackley, C. W. Cook, D. L. Plata, and K. Zhao (2014), Natural gas pipeline leaks across Washington, D. C, *Environ. Sci. Technol.*, *48*, 2051–2058.

Jeffrey, A. W. A., et al. (1991), Geochemistry of Los Angeles Basin oil and gas systems, in *Active Margin Basins*, *Mem.*, vol. 52, edited by K. T. Biddle, pp. 197–219, Am. Assoc. Petrol. Geol., Tulsa, Okla.

Jeong, S., Y.-K. Hsu, A. E. Andrews, L. Bianco, P. Vaca, J. M. Wilczak, and M. L. Fischer (2013), A multitower measurement network estimate of California's methane emissions, *J. Geophys. Res. Atmos.*, *118*, 11,339–11,351, doi:10.1002/jgrd.50854.

Kirchstetter, T. W., B. C. Singer, R. A. Harley, G. R. Kendall, and W. Chan (1996), Impact of oxygenated gasoline use on California light-duty vehicle emissions, *Environ. Sci. Technol.*, *30*, 661–670.

Kirschke, S., et al. (2013), Three decades of global methane sources and sinks, *Nat. Geosci.*, *6*, 813–823.

Kort, E. A., J. Eluszkiewicz, B. B. Stephens, J. B. Miller, C. Gerbig, T. Nehrkorn, B. C. Daube, J. O. Kaplan, S. Houweling, and S. C. Wofsy (2008), Emissions of CH_4 and N_2O over the United States and Canada based on a receptor-oriented modeling framework and COBRA-NA atmospheric observations, *Geophys. Res. Lett.*, *35*, L18808, doi:10.1029/2008GL034031.

Lamb, B. K., S. L. Edburg, T. W. Ferrara, T. Howard, M. R. Harrison, C. E. Kolb, A. Townsend-Small, W. Dyck, A. Possolo, and J. R. Whetstone (2015), Direct measurements show decreasing methane emissions from natural gas local distribution systems in the United States, *Environ. Sci. Technol.*, *49*, 5161–5169.

Leifer, I., D. Culling, O. Schneising, P. Farrell, M. Buchwitz, and J. P. Burrows (2013), Transcontinental methane measurements: Part 2. Mobile surface investigation of fossil fuel industrial fugitive emissions, *Atmos. Environ.*, *74*, 432–441.

Marcotullio, P. J., A. Sarzynski, J. Albrecht, N. Schulz, and J. Garcia (2013), The geography of global urban greenhouse gas emissions: An exploratory analysis, *Clim. Change*, *121*, 621–634.

Miller, S. M., et al. (2013), Anthropogenic emissions of methane in the United States, Proc. Natl. Acad. Sci. U.S.A. [Available at www.pnas.org/cgi/doi/10.1073/pnas.1314392110.]

Myhre, G., et al. (2013), Anthropogenic and natural radiative forcing, in *Climate Change 2013: The Physical Science Basis. Contribution of Working Group I to the Fifth Assessment Report of the Intergovernmental Panel on Climate Change*, edited by T. F. Stocker et al., pp. 710–716, Cambridge Univ. Press, Cambridge, U. K., and New York.

Newman, S., et al. (2013), Diurnal tracking of anthropogenic CO2 emissions in the Los Angeles Basin megacity during spring 2010, *Atmos. Chem. Phys.*, *13*, 4359–4372.

Novelli, P. C., and K. A. Masarie (2013), Atmospheric carbon monoxide dry air mole fractions from the NOAA ESRL carbon cycle cooperative global air sampling network, 1988–2012, Version: 2013-06-18. [Available at ftp://aftp.cmdl.noaa.gov/data/trace_gases/co/flask/surface/co_kum_surface-flask_1_ccgg_event.txt.]

Peischl, J., et al. (2013), Quantifying sources of methane using light alkanes in the Los Angeles Basin, California, *J. Geophys. Res. Atmos.*, *118*, 4974–4990, doi:10.1002/jgrd.50413.

Petron, G., et al. (2012), Hydrocarbon emissions characterization in the Colorado Front Range: A pilot study, *J. Geophys. Res.*, *117*, D04304, doi:10.1029/2011JD016360.

Phillips, N. G., R. Ackley, E. R. Crosson, A. Down, L. R. Hutyra, M. Brondfield, J. D. Karr, K. Zhao, and R. B. Jackson (2013), Mapping urban pipeline leaks: Methane leaks across Boston, *Environ. Pollut.*, *173*, 1–4.

Rudolph, J. (1995), The tropospheric distribution and budget of ethane, *J. Geophys. Res.*, *100*, 11,369–11,381, doi:10.1029/95JD00693.

Shindell, D., et al. (2012), Simultaneously mitigating near-term climate change and improving human health and food security, *Science*, *335*, 183–189.

Southern California Gas Company (2011), Pipeline safety activities performed by Southern California gas company within the County of Los Angeles report, County of Los Angeles Department of Public Works, Los Angeles, Calif.

Tennyson, M. (2005), Growth history of oil reserves in major California oil fields during the twentieth century U.S. Geol. Surv. Bull. 2172-H., Reston, Va.

Townsend-Small, A., S. C. Tyler, D. E. Pataki, X. Xu, and L. E. Christensen (2012), Isotopic measurements of atmospheric methane in Los Angeles, California, USA: Influence of "fugitive" fossil fuel emissions, *J. Geophys. Res.*, *117*, D07308, doi:10.1029/2011JD016826.

U.S. Environmental Protection Agency (US EPA) (2014), Inventory of U.S. greenhouse gas emissions and sinks: 1990–2012 Publ. EPA 430-R-14-003, Washington, D. C.

Vutukuru, S., R. J. Griffin, and D. Dabdub (2006), Simulation and analysis of secondary organic aerosol dynamics in the South Coast Air Basin of California, *J. Geophys. Res.*, *111*, D10S12, doi:10.1029/2005JD006139.

Wennberg, P. O., et al. (2012), On the sources of methane in the Los Angeles atmosphere, *Environ. Sci. Technol.*, *46*, 9282–9289.

Wong, K. W., D. Fu, T. J. Pongetti, S. Newman, E. A. Kort, R. Duren, Y.-K. Hsu, C. E. Miller, Y. L. Yung, and S. P. Sander (2015), Mapping CH_4: CO_2 ratios in Los Angeles with CLARS-FTS from Mount Wilson, California, *Atmos. Chem. Phys.*, *15*, 241–252.

Wunch, D., P. O. Wennberg, G. C. Toon, G. Keppel-Aleks, and Y. G. Yavin (2009), Emissions of greenhouse gases from a North American megacity, *Geophys. Res. Lett.*, *36*, L15810, doi:10.1029/2009GL039825.

Xiao, Y., J. A. Logan, D. J. Jacob, R. C. Hudman, R. Yantosca, and D. R. Blake (2008), Global budget of ethane and regional constraints on U.S. sources, *J. Geophys. Res.*, *113*, D21306, doi:10.1029/2007JD009415.

Yacovitch, T. I., et al. (2014), Demonstration of an ethane spectrometer for methane source identification, *Environ. Sci. Technol.*, doi:10.1021/es501475q.

York, D., N. Evensen, M. Martínez, and J. Delgado (2004), Unified equations for the slope, intercept, and standard errors of the best straight line, *Am. J. Phys.*, *72*(3), 367–375.